Article

# Self-assembled cationic #-cyclodextrin nanostructures for siRNA delivery

Raghvendra Pratap Singh, Tania Hidalgo, Pierre-Andre Cazade, Raphael Darcy, Michael Cronin, Irina Dorin, Caitriona M. O'Driscoll, and Damien Thompson

*Mol. Pharmaceutics*, **Just Accepted Manuscript** • DOI: 10.1021/acs.molpharmaceut.8b01307 • Publication Date (Web): 05 Feb 2019

# Self-assembled cationic β-cyclodextrin nanostructures for siRNA delivery

Raghvendra Pratap Singh[1$], Tania Hidalgo[2$], Pierre-Andre Cazade[1], Raphael Darcy[2], Michael F. Cronin[2], Irina Dorin[3], Caitríona M. O'Driscoll[2*], Damien Thompson[1*]

[1]Department of Physics, Bernal Institute, University of Limerick, V94 T9PX Limerick, Ireland

[2]School of Pharmacy, Cavanagh Pharmacy Building, University College Cork, Cork, Ireland

[3]Malvern Panalytical Ltd. Grovewood Road, Malvern, Worcestershire, WR14 1XZ, UK

[$]These authors contributed equally to this work

*Corresponding author: damien.thompson@ul.ie; caitriona.odriscoll@ucc.ie

**Keywords:** siRNA, Gene Delivery, Cyclodextrin, Self-Assembly, Molecular Dynamics

**Table of Content Graphic:**

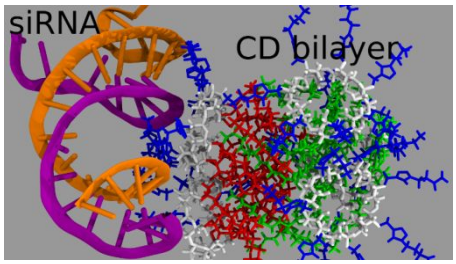


## Abstract

Functionalised cyclodextrin molecules assemble into a wide variety of superstructures in solution, which are of interest for drug delivery and other nanomaterial and biomaterial applications. Here we use a combined simulation and experimental approach to probe the co-assembly of siRNA and cationic cyclodextrin (c-CD) derivatives into a highly stable gene delivery nanostructure. The c-CD form supramolecular structures *via* interdigitation of their aliphatic tails, analogous to the formation of lipid bilayers and micelles. The native conformation of siRNA is preserved by the encapsulating c-CD superstructure in an extensive hydrogen bonding network between the positively charged sidearms of c-CD and the negatively charged siRNA backbone. The stability of the complexation is confirmed using isothermal titration calorimetry, and the experimental/simulation co-design methodology opens new avenues for creation of highly-engineerable gene delivery vectors.

## Introduction

Gene silencing *via* RNA interference (RNAi) using short (~20-25 nucleotides) double-stranded RNA (siRNA)[1-14], provides the opportunity to design a new generation of therapeutics capable of treating a wide range of diseases including those with high unmet needs such as brain cancers and neurodegenerative disorders[12, 15-17]. Following parenteral administration, nucleases in the blood and at the cellular level degrade siRNA[18], which compromises the effectiveness of the nucleic acid based

therapeutics[16-17]. However, the small size and relative simplicity of siRNA (compared to complete RNA or DNA[19]) provides opportunities for targeting of the biomolecule by nanoparticle-based delivery[3-4, 6-8, 10, 20-23]. Both organic (lipid-based[8, 12] or otherwise) and inorganic carriers[12, 18-19, 24-25] increase the permeability of the cellular membrane and deliver siRNA to the target site. While brain delivery remains a major challenge, knowledge of the self-assembly properties of a gene delivery vector and of its complexation with nucleic acids may enhance understanding of its interactions with living cells. In particular, cationic lipid-based nanovectors form tightly-bound complexes with siRNA which translocate through the phospholipid bilayer. Although some progress has been made, the major barrier to clinical translation of this method is the lack of nontoxic, effective delivery systems that can be manufactured to consistent quality, ensuring delivery to the diseased site and achieving the required duration of activity[26].

To date, the delivery problem has been tackled using viral and non-viral approaches. Viral technologies for nucleic acid delivery are remarkably effective and have made significant progress, with several FDA approved products including CAR-T cell therapy (Novartis) for treatment of paediatric relapsed/refractory (r/r) B-cell acute lymphoblastic leukaemia (ALL), and Luxturna™ (voretigene neparvovec) for treatment of vision loss due to confirmed biallelic RPE65-mediated inherited retinal dystrophies (Spark Therapeutics). In contrast, development of non-viral approaches has lagged behind[27]. However the recent design and synthesis of biocompatible materials capable of producing nano-complexes with nucleic acids has resulted in more promising clinical data and it is anticipated at time of writing in December 2018 that the first non-viral RNAi therapeutic using a lipid-based nanoparticle formulation for liver disease (www.alnylam.com) will reach the market in the coming year.

Among a variety of nanocarriers, the potential of cyclodextrin (CD) molecules[19, 21] as promising delivery platforms for therapeutic oligonucleotides has been well established[28]. Cyclodextrins are a biocompatible family of cyclic oligosaccharides with hydrophilic primary and secondary faces and a hydrophobic cavity. The presence of hydroxyl groups on the ring structure allows modifications with different functional groups, giving rise to a library of compounds including amphiphilic, cationic, anionic, PEGylated and targeted CDs[28-29]. Co-formulation of selected CD derivatives has resulted in the design of 'bespoke' nanoparticles loaded with nucleic acid for targeting to specific disease sites[30-32]. These modified CDs have successfully delivered both plasmid pDNA[33-34] and siRNA by enhancing cellular uptake, promoting endosomal release resulting in significant levels of transfection and gene knockdown[26-27]. For example, a 70nm cyclodextrin-based nanoparticle can package ~2000 siRNA molecules in a 20:1 ratio for targeted delivery[7, 10]. Proof of concept has also been shown *in vivo* in animal models of prostate cancer[20], Huntington's disease[35] and

inflammatory bowel disease (IBD)[36]. More recently, antibody targeted CD nanoparticles have shown gene silencing and therapeutic efficacy in blood from adult acute myeloid leukaemia AML patients[37]. Preliminary toxicity studies *in vitro* and *in vivo* have confirmed the safety of these CDs[38].

Initial characterisation studies have elucidated the physicochemical properties and the molecular alignment in CD-based nanocomplexes. Routinely the size, charge and shape of NPs, essential parameters known to influence therapeutic activity, are monitored using techniques including dynamic light scattering (DLS), zeta potential measurements, electron and atomic force microscopy. For example, the self-assembly properties of two cationic amphiphilic cyclodextrins (C16 *vs*. C12 alkylthiol lipid chain lengths) following complexation with DNA have been investigated using small angle X-ray scattering (SAXS) to probe the structure of the complexes and locate DNA within them[39]. The cyclodextrin with the longer C16 lipid chain formed multi-lamellar nano-assemblies with DNA bound between the two polar layers of the CD protonated amino groups in alternation with the lipid bilayers. In contrast, the cyclodextrin with the shorter lipid chain forms micelles, which aggregate into clusters following electrostatic interaction with DNA. These results indicate that the hydrophobic-hydrophilic balance between the two faces of cationic amphiphilic cyclodextrins modulated the structures of complexes formed with nucleic acids. Finally, circular dichroism has been used to monitor the conformational changes of DNA and RNA in cyclodextrin complexes[40]. Although siRNA was more susceptible than DNA to conformational changes, complexation with CDs had a stabilizing effect that maintained the A-form secondary structure essential for gene silencing. In addition, factors such as temperature and pH were shown to influence the conformation of the nucleic acids, which may be relevant considerations for processing and manufacture.

In summary, the supramolecular structure of RNA-carrier complexes has been shown to influence therapeutic performance and stability during manufacture, storage and following exposure to biological fluids. Non-viral nanocomplexes are likely to be multi-component formulations necessary to overcome the complex *in vivo* barriers to delivery. Therefore, it is essential to characterize in as much detail as possible the nature of interactions with the encapsulated nucleic acids. The aim of this work is to use molecular dynamics computer simulations in tandem with isothermal titration calorimetry (ITC) to advance our knowledge of CD-nucleic acid interactions[41-42], to help toward identifying the optimum design features required to maximize performance and minimize toxicity.

## Methods

Molecular dynamics computer simulations: In this study, we used state of the art molecular dynamics

(MD) computer simulations to model the dynamic encapsulation of siRNA *via* templated self-assembly of β-cyclodextrin derivatives on the siRNA surface. 21-base pair siRNA molecular models were built using A-DNA PDB structures as templates (5IYE[43], 5MVT, 5MVQ[44], 5OKL[45], 3V9D[46]), and the uracil nucleobases were modified to 2'-o-methyluridine at 4 positions. Click-propyl-amine cationic β-cyclodextrin models were generated from published molecular structures[28, 30, 47]. Each complex was solvated in TIP3P[48] water in a cubic box of edge length 18 nm and any net charge was neutralized by adding background $Na^+$ and $Cl^-$ ions. All studies were carried out employing periodic boundary conditions with Particle Mesh Ewald method[49] to treat long-range electrostatics. High frequency bonds to hydrogen were constrained using the LINCS algorithm[50] which allowed the use of a two femtosecond (2 fs) time step to integrate the equations of motion. The simulation cells were equilibrated and thermalized[51-52] over 10 ns of molecular dynamics to obtain a stable constant pressure-temperature (NPT) ensemble at 1 atm and 300K. Force field parameters for cationic β-cyclodextrin (CD)[51-52] were derived using the Charmm generalized force field (CgenFF)[53] for small molecule parameterization. This modified version of the Charmm36 force field[54-57] was used to simulate the solvated siRNA-CD complexes with the Gromacs MD code version 2016-beta2[58-59]. We first simulated the formation of a stable complex between siRNA and single β-cyclodextrin and cationic β-cyclodextrin (cCD) molecules and then modelled the interaction of siRNA with multiple β-cyclodextrins (native CD and cCD) at mass ratio of up to 1:10.

Isothermal titration calorimetry experiments: All experimental measurements were carried out using the MICROCAL™ PEAQ-ITC (Malvern Panalytical Ltd., United Kingdom). A solution of 100 μM of the Click propyl-amine CD was loaded into the syringe and the nucleic acid (siRNA at 10 μM) deposited in the sample cell, in both cases at pH 6. Trifluoroacetate was also present as a counter-ion. The reference cell was loaded with ultra-pure RNAse-free water. After a 60-second delay and an initial injection of 0.4 μL (to negate diffusion effects) a typical experiment involved a series of 19 injections of 2 μL of the titrant solution into the cell. The sample cell was stirred at 750 rpm throughout the experiment and the experimental temperature was maintained at 25°C. The feedback/gain mode was set to low. The area under the peak of the resulting heat profile was integrated, normalized by the concentrations, and plotted against the molar ratio of ligand to protein using MicroCal PEAQ-ITC analysis software. The resulting binding isotherms were fitted by nonlinear regression using a one set of sites model to yield the stoichiometry of the interaction (n), the equilibrium dissociation constant ($K_D$), and the change in enthalpy ($\Delta H$). The Gibbs free energy change ($\Delta G$) was calculated from $\Delta G = -RT \ln K_D$ and the entropy ($\Delta S$) from $\Delta G = \Delta H - T\,\Delta S$.

## Results and Discussion

The dynamical self-assembly behaviour of β-cyclodextrin (CD) derivatives around siRNA was investigated using classical MD simulations in water at ambient temperature (300K). The data confirms the structural stability of siRNA under physiological conditions and shows that siRNA templates its encapsulation *via* the self-assembly of cationic amphiphilic β-cyclodextrin (cCD) molecules into a cloaking bilayer. Our computed high complex stability is confirmed using experimental ITC measurements.

Computed structure, dynamics and energetics of siRNA/CD and siRNA/cCD complexes: For a better understanding of the complexation process, we performed multiple unbiased MD simulations of siRNA/CD and siRNA/cCD complexation, starting from completely unbound conformations with siRNA and the host molecules well separated in water. The simulations were performed at ambient temperature, and structures were initially sampled for 200 ns for single CD complexes and multi-CD complexation in a siRNA:CD mass ratio of 1:10 (1:120 for CD and 1:39 molecules for the cCD). The simulations where extended up to 1 μs when necessary. In addition, control simulations (200 ns each) of siRNA alone in water and also CD (native and cCD) dimerization alone in water were performed, to compare with the calculated CD/siRNA complexes.

The simulations of siRNA alone and complexed to a single native CD or cCD unit confirm that siRNA is stable in water at ambient conditions, as deduced from computed structural parameters including Radius of Gyration (Rg), Root Mean Square Deviation (RMSD), and Root Mean Square Fluctuations (RMSF). Computed Rg values highlight the compactness of siRNA, averaging 19.0 ± 0.2 nm for all, which is close to the known B-DNA Rg value. The RMSD of uncomplexed siRNA (Figure 1A) ranges between ~0.1 and 0.6 nm. The modest increase in RMSD of siRNA with complexed CD suggests, in agreement with similar studies[60], that the structure of siRNA is not significantly altered by CD. This is confirmed by the scan of RMSF values across the 42-base RNA molecule (Figure 1B) which shows that molecular fluctuation in siRNA is localised at the ends of the duplex. Terminal base-fraying is inhibited in the siRNA/cCD complex because the cCD molecule targets one of the terminal base-pairs. Such nanovector-mediated preservation of the native siRNA molecular structure is a potentially useful design principle in that it may increase the ability of siRNA to perform its designated function *in vivo*. Having confirmed the stability of siRNA in our model, we present below details of the molecular mechanism of self-assembly of siRNA nanovectors from cCD molecules.

The binding complex between siRNA and unfunctionalised CD(1:1) shows very specific interaction modes of CD with the major groove of siRNA (Figure 2). It shows two primary binding modes as previously shown by Manzanares *et al*.[61] The first can be described as perpendicular

insertion of CD into the major groove, sandwiched between two strands (Figure 2A). The second binding mode is laterally aligned full CD interaction with the siRNA backbone (Figure 2B). The first binding mode persists for ~70ns simulation time before switching to the second binding mode. The insertion of CD in the major groove modulates the structural dynamics of siRNA with a minor localized widening of the major groove (Figure 2C), hence comparatively higher fluctuation (Figure 1) in RMSD (from ~40-90ns) and RMSF (4-terminal base pairs) data.

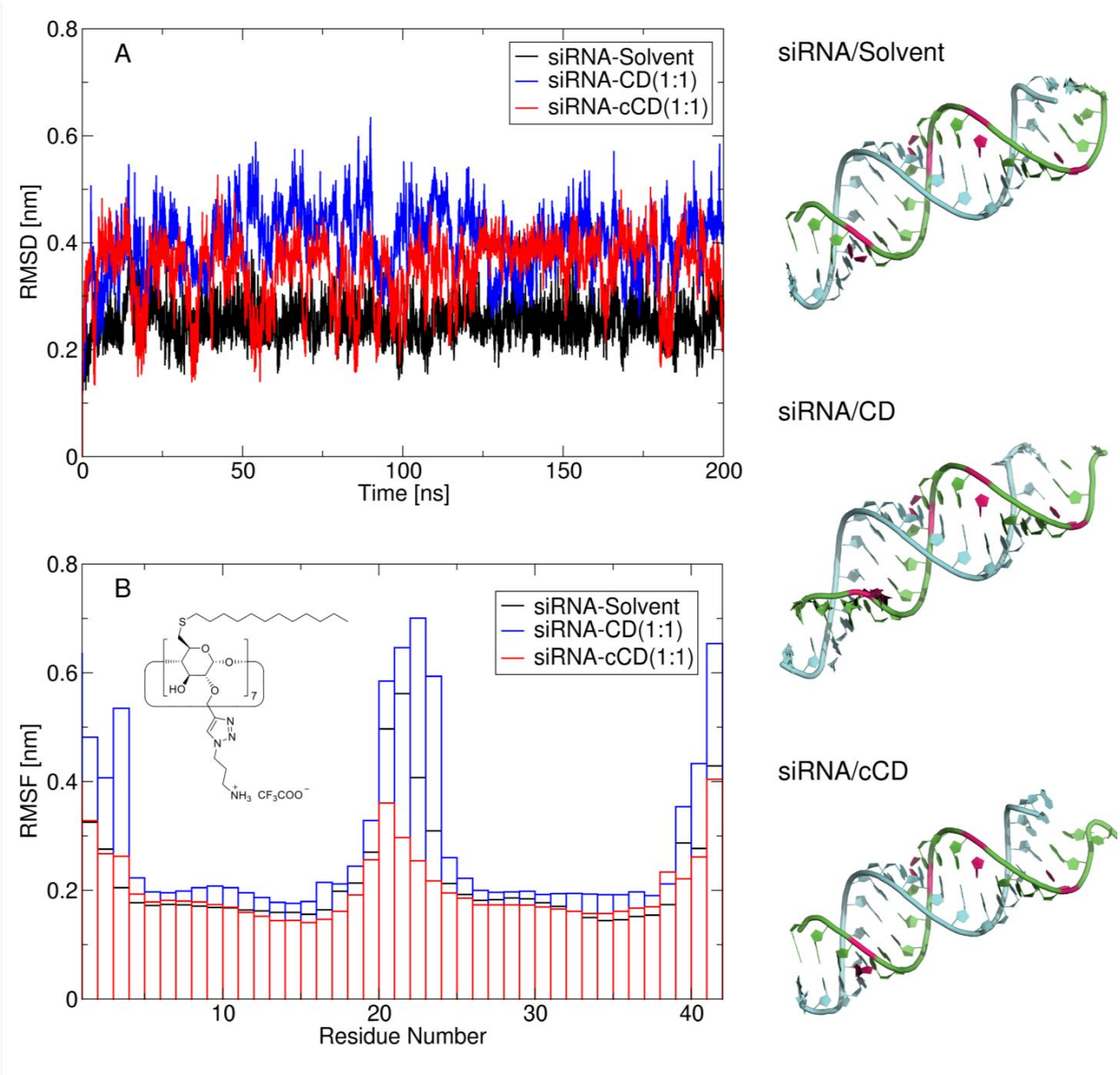


**Figure 1** A comparison of the computed dynamics of siRNA (Root Mean Square Deviation [A] and Root Mean Square Fluctuation [B]) in solution and complexed with native CD and cationic cCD (1:1). The molecular structure of c-CD, heptakis[2-O-(N-(3″-aminopropyl)-1′H-triazole-4′-yl-methyl)-6-dodecylthio]-β-cyclodextrin trifluoroacetat (Click-CD, MW: 4191 g/mol) is shown in the inset of panel B. Computed average siRNA conformations are shown on the right.

Upon introducing a second CD, CD−CD dimerization competes with CD−siRNA binding and so only transient, non-specific CD−RNA binding modes are observed (Figure 2D-F). At the higher CD concentration, siRNA is mostly a simple solvated structure with very little deviation from the starting equilibrated conformation. When complexed to siRNA, CD forms on average two hydrogen bonds per molecule which gives small decreases in base-pair hydrogen bond populations.

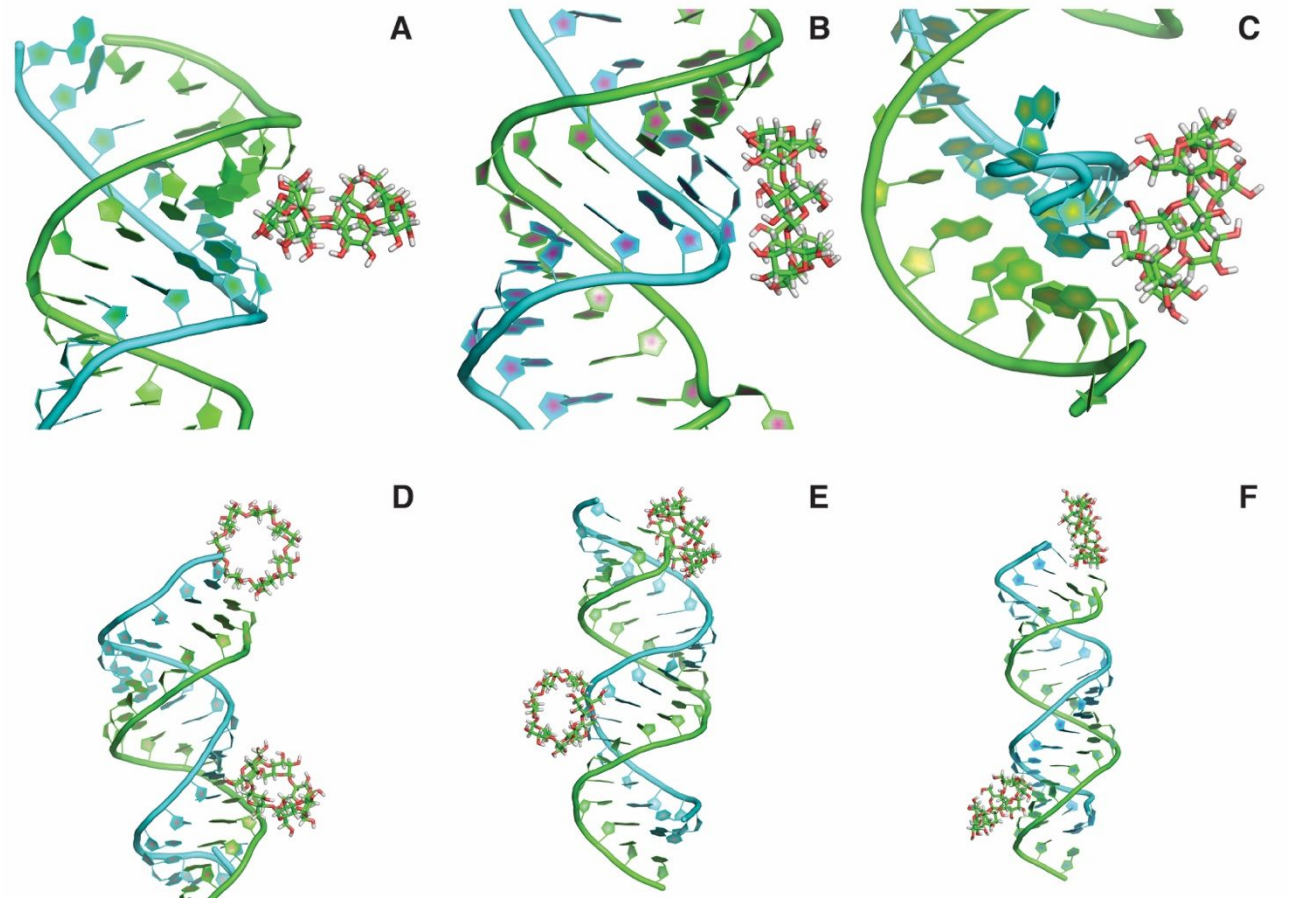


**Figure 2** Computed preferred binding modes of unmodified CD to siRNA(1:1 [A-C] and 1:2 [D-F]).

By contrast, siRNA is more stable when complexed to cCD. The cCD molecule interacts with the siRNA backbone *via* its cationic amino groups (Figure 3). cCD walks along the backbone and anchors tightly on the terminal base-pair at one end of siRNA, where it remains for the duration of the simulation. Upon insertion of a second cCD, similar interaction occurs with the backbone of siRNA with no dimerization between the charged cCD molecules. The second cCD molecule binds to the middle of the siRNA, splaying across the major groove. The end-bound cCD molecule forms on average five H-bonds to siRNA and the second CD forms ten H-bonds. These results are in good agreements with simulations performed on chitosans which show that the encapsulation of DNA

strands depends on both the charge of the functionalized group and on the number of H-bonds a vector can form with DNA/siRNA[62].

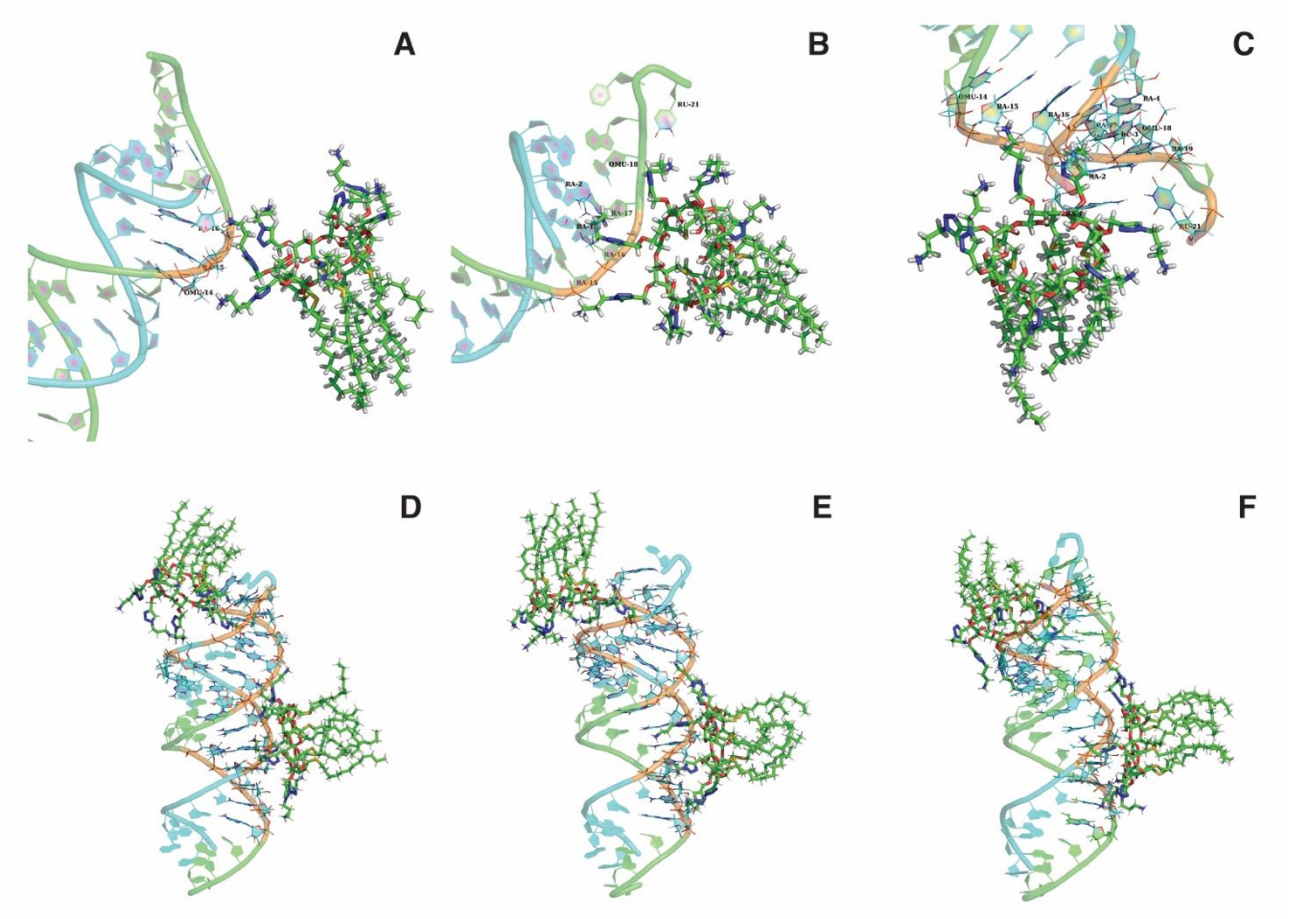


**Figure 3** Computed preferred binding modes of cCD to siRNA(1:1[A-C] and 1:2[D-F]).

Computed self-assembly on CD-based nano-vectors around siRNA: On increasing the siRNA/CD mass ratio to 10 (1:120 molecules), the native CD molecules formed mostly native dimer configurations with a small population also of tetramers. These higher order CD structures interacted with siRNA but without any specific assembly of the units on siRNA surface during the 0.5 μs simulations. The interactions among siRNA and CD do not significantly alter the siRNA (Figure 4A,B), as the number of H-bonds oscillates between 5 and 10 per CD (**Error! Reference source not found.**C) to give very short lived and non-specific complexation (Figure 4D). One large cluster of loosely-bound CD dimers persists for few hundred nanoseconds at one terminus during the simulation, but still no specific pattern of assembly emerges from analysis of the CD-CD and CD-siRNA contacts, indicating that at high concentration unmodified CD simply aggregates non-specifically on siRNA. The assembly reduces the solvent accessible surface area (SASA) of siRNA and ~80 H-bonds to water are lost as the siRNA to sugar H-bonding increases 6-fold (compared with native CD) to make

a tight, specific electrostatically-bound complex (Figure 4C,D). The partial or total coverage of siRNA by cationic vectors including cylodextrins, chitosans, PGA, PMAL and PAMAM, with corresponding reduction of solvent accessibility to the nucleotides, has been observed in various experimental and modelling studies and is essential to preserve the stability of the siRNA and allow it to cross the cell lipid membrane.[60-66]

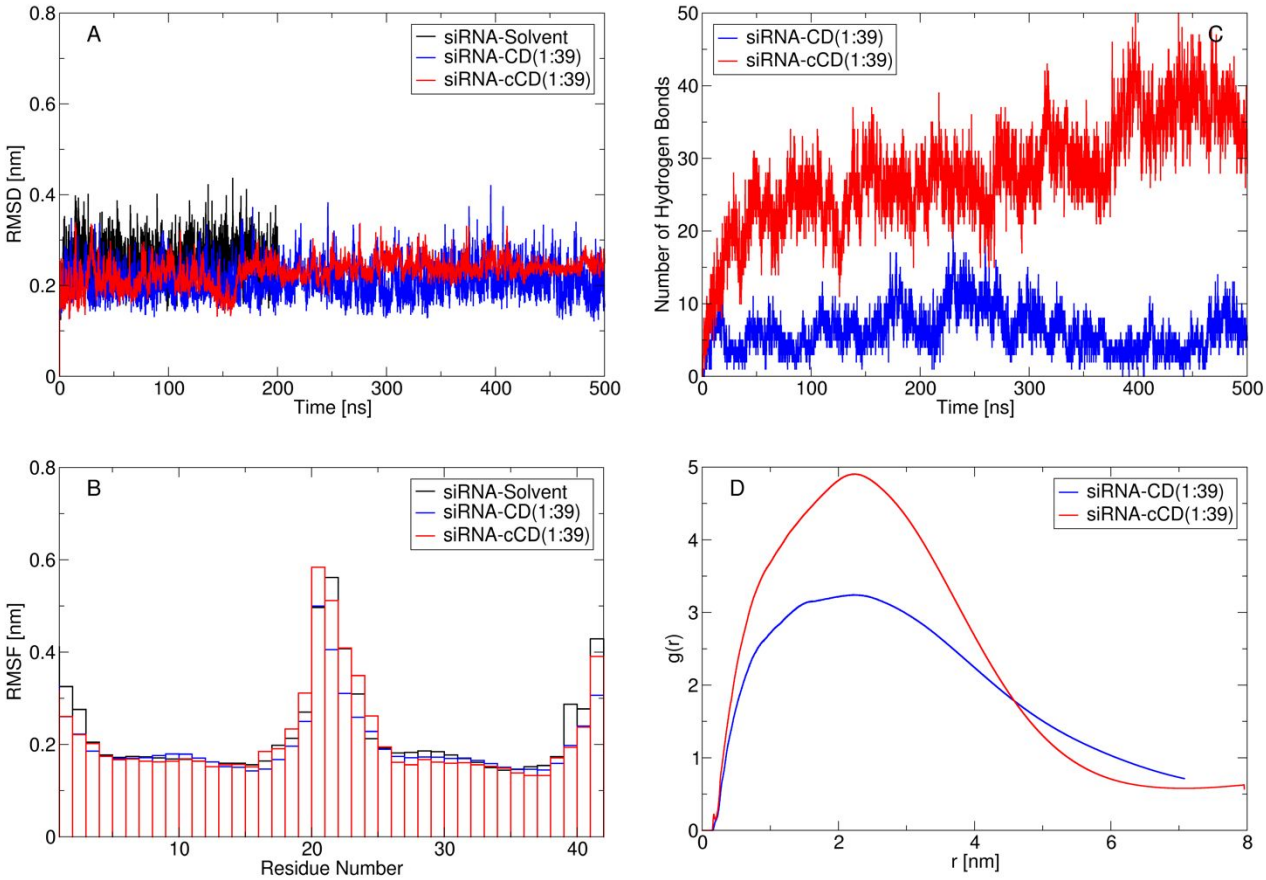


**Figure 4** Comparison of the computed properties of siRNA/CD and siRNA/cCD complexes assembled at a mass ratio of 10. [A] RMSD, [B] RMSF per residue, [C] hydrogen bonding between siRNA and CD/cCD, and [D] radial distribution of CD/cCD from the siRNA center of mass.

By contrast, cCD dimers formed in the very early stages of the simulation condense into multimeric units on the surface of siRNA (Figure 5). The cCD molecules use their cationic termini to anchor to the negatively charged nucleic acid bases and form multimeric supramolecular structures along the backbone. The cationic groups dangle in the major groove of the siRNA, which generates a pull that causes fraying of one terminal base-pair (residues 21 and 22) at one end of siRNA, as reflected in the rise in RMSF (**Error! Reference source not found.**B). This is the only change in the physical and structural parameters of siRNA as the encapsulating cCD superstructure assembles around it. The cCD molecules form dimers and then these dimers associate into larger assemblies, showing behaviour analogous to biological lipids due to the cationic modification at one face of the

CD ring and the long hydrophobic aliphatic chains on the other face. The cCD molecules stack together *via* interdigitation of the aliphatic chains and the charged head groups at each end anchor either to the negatively charged nucleic acid backbone or face out into solvent. This type of association into bilayer patches creates a hydrophobic core and positively charged head groups create the external boundaries of the bilayer, mimicking natural lipid bio-membranes. This type of multi-lamellar nano-assembly was previously observed in the case of DNA complexed with our modified CDs[39]. The largest assembly observed during the simulations comprised a hexamer of six cCD molecules on the surface of nucleic acid, while three other secondary assemblies also form on the surface of the nucleic acid backbone containing 4-6 cCD molecules at a time.

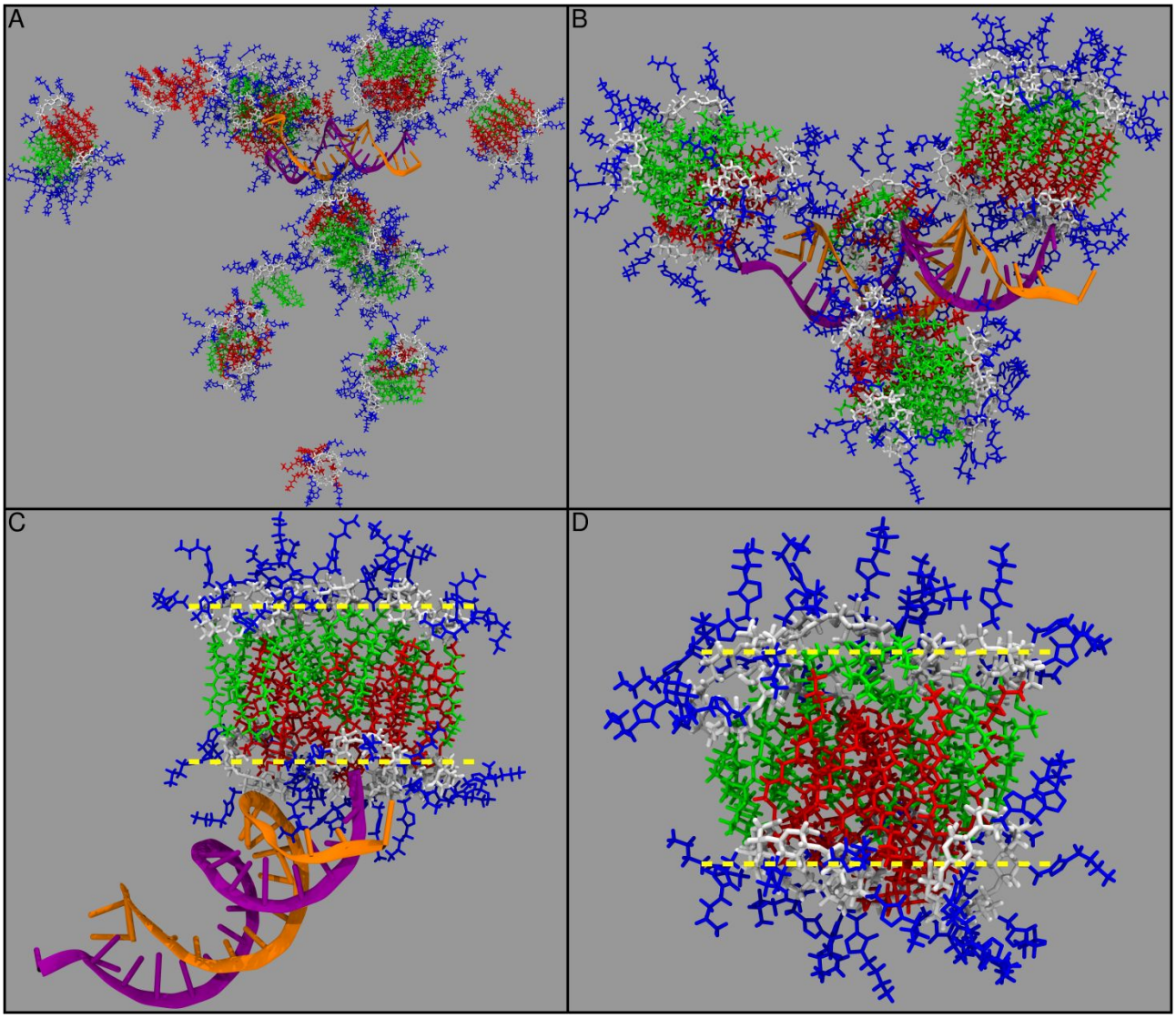


**Figure 5** Representative computed self-assembled multimeric units of 39 cCD molecules around siRNA. Panel (A) shows how the originally randomly distributed cCD converge towards the siRNA. Panel (B) illustrates formation of cCD clusters at the three main interaction points of the siRNA, the two ends and in the middle around a major groove. (C) Assembly of a 6 cCD molecule bilayer structure at one end of siRNA. Dashed yellow lines mark the CD ring alignment. (D) Formation of a 6 cCD molecule bilayer in water. The cationic sidearms of cCD are coloured blue, the central sugar

rings are coloured white and the interdigitating aliphatic chains are coloured red and green to distinguish the first and second layer in the assembly.

The free cCD molecules in the solvent are rarely in a single unit conformation, but instead exist in dimer, trimer, tetramer and occasionally pentameric/hexameric assemblies. The rapid assembly of cCD on the surface of siRNA suggests that these modified CDs have biological lipid-like self-assembly behaviour, encapsulating siRNA in a stable electrostatically bound carrier which does not significantly affect the overall average structural properties of the siRNA molecule, as required for the design of nano-vectors for targeted delivery of nucleic acid and other small (charged, hydrophilic) drug molecules. The maintenance of the structural intergrity of siRNA in the cCD complex is consistent with previously published circular dichroism results[40]. The H-bond profiles of siRNA/CD and siRNA/cCD (**Error! Reference source not found.**C) clarifies the improved assembly behaviour obtainable with cCD, as the cCD molecules assemble into bi-layered structures with 6-fold increase (compared with native CD) in electrostatic interactions with siRNA. The pronounced peak in the computed radial distribution function for cCD (**Error! Reference source not found.**D) indicates specific assembly of ordered cCD structures on the surface of siRNA, while unmodified CD shows a broader, less featured distribution reflecting weaker, less specific, shorter-lived interactions with siRNA.

A more detailed analysis of the assemblies is shown in **Error! Reference source not found.**. Aggregation proceeds by growing the average cluster sizes (Fig. 6A) while reducing the overall number of clusters. Evidence of siRNA-templated assembly is provided for the three aggregates that make electrostatic contact with the siRNA surface (Fig. 6B) as they account for most of the assemblies of four or more cCD molecules. These aggregates show a tendency to coalesce further eventually forming a bilayer around siRNA. The experimentally-validated model for specific, electrostatic interaction between cCD and siRNA suggests a mechanism for templated assembly starting with the adhesion of few molecules at well-defined sites that serve as anchoring points for the self-assembly of a full lipid bilayer-like cloak around siRNA. The present microsecond trajectory captures the initial stages of this evolving structure with many cCD dimers and even tetramers still in suspension in the solvent. The largest assembly covers approximately 70% surface of the siRNA and uses 50% of available cCD molecules. Future work will involve extending to longer sampling times (using coarse grained models and metadynamics) and increasing concentrations of cCD, which may help further clarify the balance between cCD multimerisation and cCD−RNA electrostatic binding in creation of the full cCD siRNA delivery particle.

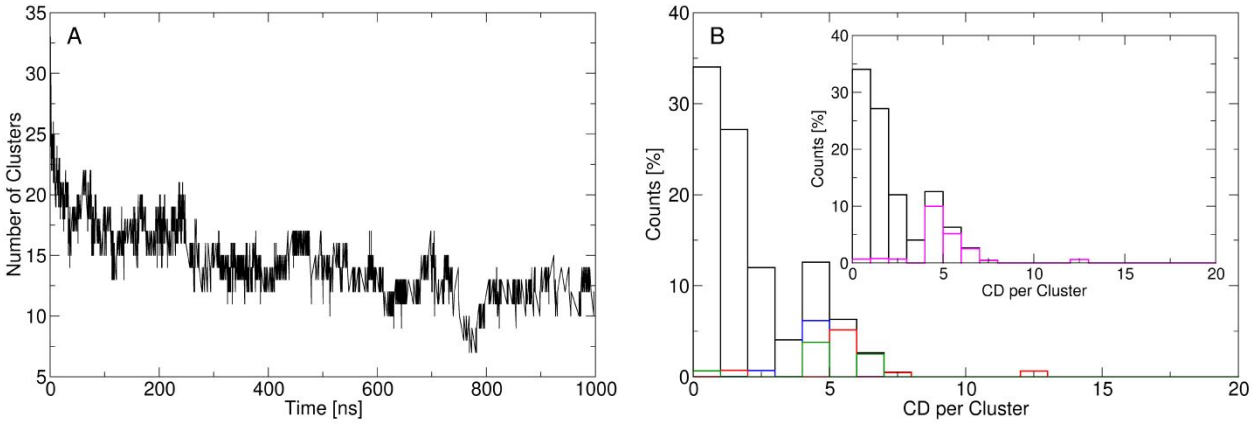


**Figure 6** Analysis of the cluster aggregates formed by cCD molecules in solution. Panel (A) shows the temporal evolution of number of clusters formed during 1 μs of dynamics. Panel (B) shows the distribution of the number of cCD molecules per cluster: black represents all the aggregates, and blue, red and green represent the three aggregates coating siRNA. The inset shows the same information with the contributions of the three siRNA-binding clusters summed in the magenta histogram.

Experimental proof-of-concept testing of the predicted complexes: To investigate cCD complexation with a nucleic acid aqueous suspension of siRNA, we used ITC to quantify the heat released or absorbed during complexation. These measurements allowed us to confirm the type of interaction and estimate the energies produced during the binding process. In a typical ITC experiment, aliquots of a concentrated solution of cyclodextrins are added in a time-controlled manner to a cell containing the interacting molecule, which is maintained at constant temperature. During cyclodextrin addition, the two materials interact and the observed released heat is directly proportional to the amount of binding compound added with the solution aliquot. The molecular structure of c-CD is given in Figure 1B above and the negative control non-silencing siRNA has sense strand sequence 5'-UUC UCC GAA CGU GUC ACG UdT dT-3 (siRNA Universal Negative Control (SIC001, Sigma, MW: 13,300 g/mol). Parameters measured from ITC are given in Table 1 below (Figure 6).

**Table 1 Thermodynamics of the guest:host interaction between siRNA (10 μM of 20-25 nucleotide long double-strands) and c-CD (100 μM) in deionised water at 25.1 °C.**

| **[Syringe: c-CD] [Sample Cell: siRNA]** | ***Stoichiometry*** ±std. dev. | **$K_D$ [μM]** ±std. dev. | **ΔH (kcal/mol)** ±std.dev | **ΔG (kcal/mol)** | **-TΔS (kcal/mol)** |
|---|---|---|---|---|---|
| 100: 10 μM-R1 | 0.53 ± 0.20 | 1.79 ± 0.97 | -5.69 ± 1.30 | -7.84 | -2.15 |

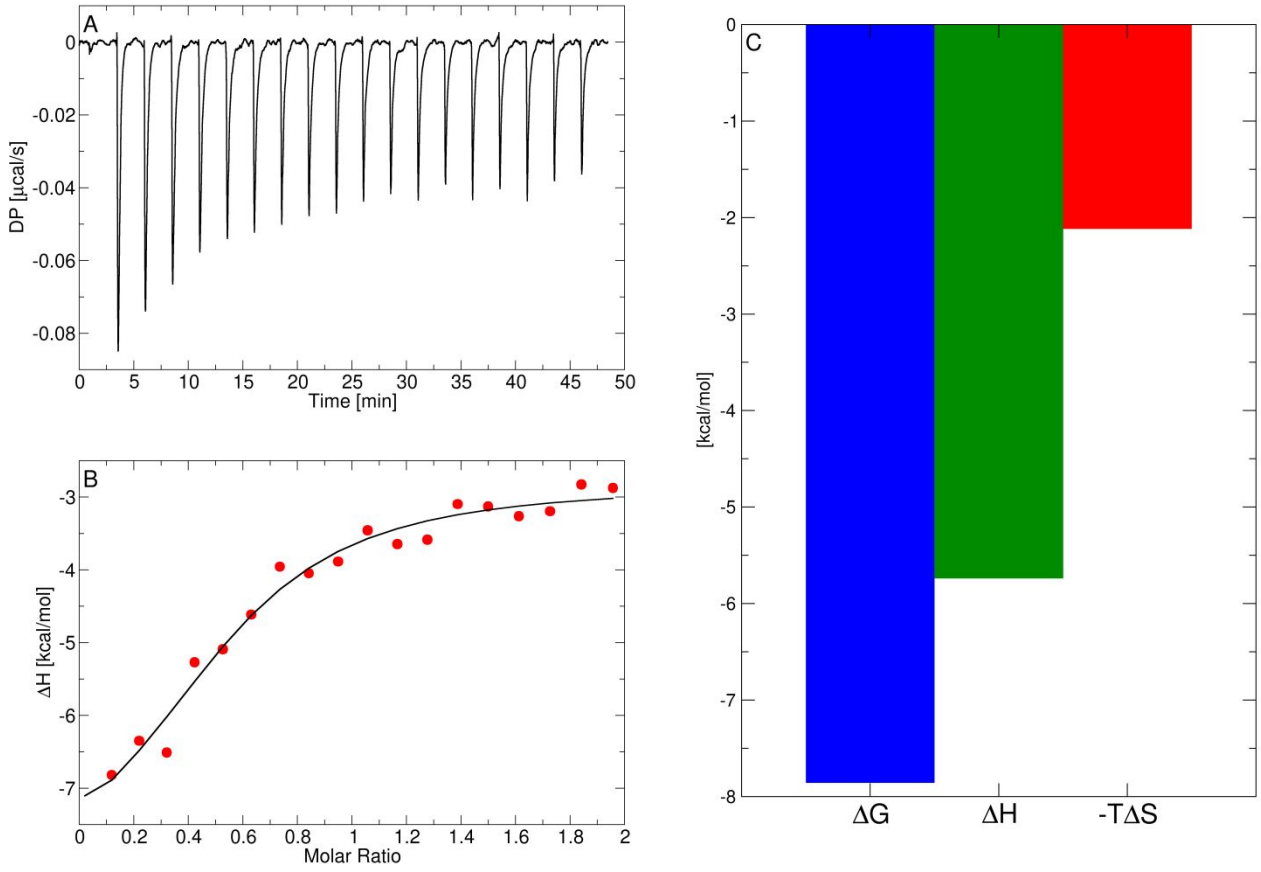


**Figure 6** Typical ITC plot. Raw plot (A), integrated heat plot (B) of complex formation between Click-CD and siRNA solution at 10 µM. The dots depict the experimental results while the continuous line depicts the fitted curve. Signature plot (C), blue = Gibb's free energy (ΔG), green = enthalpy (ΔH), red = entropic part (-TΔS).

In aqueous solution, the interaction between c-CD and siRNA is exothermic and also spontaneous and is enthalpy driven with a low dissociation value. The magnitude of the released heat decreased progressively with each injection until the full complexation process was achieved. This is most likely related to the saturation process as c-CD assembles on siRNA (Fig. 7). The experimentally measured favourable enthalpy with small entropic contribution, confirms the prediction from the MD simulations that electrostatic interactions direct the siRNA encapsulation complexation. When CD binds to the siRNA, water molecules are displaced and move into the bulk water and this is entropically favorable. While electrostatic interactions direct the cCD−siRNA complexation, weaker van der Waals and hydrophobic interactions remain important for creation of the host superstructure *via* stacking of CD ring stacking and interdigitaiton of alkyl tails.

## Conclusion

Click-CD molecules spontaneously form superstructures in solution which can assemble around

siRNA to form a stable host that stabilises siRNA *via* electrostatic interactions. We employed large-scale all-atom molecular dynamics simulations to track the assembly process and used isothermal titration calorimetry experiments to confirm the stability of the complexation between siRNA and the cCD superstructures. The negatively charged siRNA molecules serve as an ideal template around which the cationic cCD molecules rapidly assemble into stable multimers, which could provide a promising gene delivery vector. More generally, the computed structures further illustrate the lipid-like behaviour of CD derivatives in solution and their capacity to form stable supra-structures, providing nanoscale molecular templates with highly controllable shape and size complexity. The amphiphilic nature of the complex and the resulting bilayer formation will aid membrane permeability which should in turn enhance transfection activity.

**Acknowledgments**

This publication has emanated from research conducted with the financial support of Science Foundation Ireland (SFI) and is co-funded under the European Regional Development Fund under Grant Number 13/RC/2073 (Centre for Research in Medical Devices, CÚRAM**)**. DT acknowledges SFI for support under Grant Number 15/CDA/3491 and for computing resources at the SFI/Higher Education Authority Irish Center for High-End Computing (ICHEC). RPS was supported under an Enterprise Ireland (EI) innovation partnership on Advanced Biopharmaceutical Formulation. COD and TH acknowledge EU Horizon 2020 support under Marie Skłodowska-Curie grant no. 713690.

**References**

1. Haasnoot, J.; Berkhout, B., RNA interference: its use as antiviral therapy. *Handb Exp Pharmacol* **2006,** (173), 117-150.
2. Agrawal, N.; Dasaradhi, P. V. N.; Mohmmed, A.; Malhotra, P.; Bhatnagar, R. K.; Mukherjee, S. K., RNA interference: biology, mechanism, and applications. *Microbiology and molecular biology reviews : MMBR* **2003,** *67* (4), 657-685.
3. Copyright. In *Nanostructures for Drug Delivery*, Andronescu, E.; Grumezescu, A. M., Eds. Elsevier: 2017; p iv.
4. Alonso, M. J.; Csaba, N. S., *Nanostructured biomaterials for overcoming biological barriers*. Royal Society of Chemistry: 2012.
5. Arruda, D. C.; Hoffmann, C.; Charrueau, C.; Bigey, P.; Escriou, V., Innovative nonviral vectors for small-interfering RNA delivery and therapy. In *Nanostructures for Novel Therapy*, Elsevier: 2017; pp 713-740.
6. Atala, A., Re: Anisamide-Targeted Cyclodextrin Nanoparticles for siRNA Delivery to Prostate Tumours in Mice. *The Journal of urology* **2013,** *190* (1), 357.
7. Bartlett, D. W.; Davis, M. E., Physicochemical and biological characterization of targeted, nucleic acid-containing nanoparticles. *Bioconjugate chemistry* **2007,** *18* (2), 456-468.
8. Betageri, G. V.; Jenkins, S. A.; Parsons, D. L., Liposome drug delivery systems. **1993**.
9. Donglu, S., *Bio-inspired Nanomaterials and Applications: Nano Detection, Drug/gene*

*Delivery, Medical Diagnosis and Therapy*. World Scientific: 2014; Vol. 4.
10. Fitzgerald, K. A.; Malhotra, M.; Gooding, M.; Sallas, F.; Evans, J. C.; Darcy, R.; O'Driscoll, C. M., A novel, anisamide-targeted cyclodextrin nanoformulation for siRNA delivery to prostate cancer cells expressing the sigma-1 receptor. *International journal of pharmaceutics* **2016,** *499* (1-2), 131-145.
11. Ge, Q.; Evans, D.; Xu, J. J.; Yang, H. H.; Lu, P. Y., Pulmonary Delivery of Small Interfering RNA for Novel Therapeutics. *Delivery Technologies for Biopharmaceuticals* **2009**.
12. Gomes, M. J.; Dreier, J.; Brewer, J.; Martins, S.; Brandl, M.; Sarmento, B., A new approach for a blood-brain barrier model based on phospholipid vesicles: Membrane development and siRNA-loaded nanoparticles permeability. *Journal of Membrane Science* **2016,** *503*, 8-15.
13. Sadreddini, S.; Safaralizadeh, R.; Baradaran, B.; Aghebati-Maleki, L.; Hosseinpour-Feizi, M. A.; Shanehbandi, D.; Jadidi-Niaragh, F.; Sadreddini, S.; Kafil, H. S.; Younesi, V., Chitosan nanoparticles as a dual drug/siRNA delivery system for treatment of colorectal cancer. *Immunology letters* **2017,** *181*, 79-86.
14. Jana, S.; Jana, S., *Particulate Technology for Delivery of Therapeutics*. Springer: 2017.
15. Kaczmarek, J. C.; Kowalski, P. S.; Anderson, D. G., Advances in the delivery of RNA therapeutics: from concept to clinical reality. *Genome medicine* **2017,** *9* (1), 60.
16. Burnett, J. C.; Rossi, J. J., RNA-based therapeutics: current progress and future prospects. *Chemistry & biology* **2012,** *19* (1), 60-71.
17. Takahashi, M.; Han, S. p.; Scherer, L. J.; Yoon, S.; Rossi, J. J., Current Progress and Future Prospects in Nucleic Acid Based Therapeutics. **2017**.
18. Am Hong, C.; Nam, Y. S., Functional nanostructures for effective delivery of small interfering RNA therapeutics. *Theranostics* **2014,** *4* (12), 1211.
19. Petrocca, F.; Lieberman, J., Promise and challenge of RNA interference–based therapy for cancer. *Journal of Clinical Oncology* **2010,** *29* (6), 747-754.
20. Guo, J.; Ogier, J. R.; Desgranges, S.; Darcy, R.; Caitriona, O., Anisamide-targeted cyclodextrin nanoparticles for siRNA delivery to prostate tumours in mice. *Biomaterials* **2012,** *33* (31), 7775-7784.
21. Heidel, J. D.; Yu, Z.; Liu, J. Y.-C.; Rele, S. M.; Liang, Y.; Zeidan, R. K.; Kornbrust, D. J.; Davis, M. E., Administration in non-human primates of escalating intravenous doses of targeted nanoparticles containing ribonucleotide reductase subunit M2 siRNA. *Proceedings of the National Academy of Sciences* **2007,** *104* (14), 5715-5721.
22. Torchilin, P. V.; Torchilin, V. P.; Torchilin, V.; Weissig, V., *Liposomes: a practical approach*. Oxford University Press: 2003.
23. Svenson, S.; Prud'homme, R. K., *Multifunctional nanoparticles for drug delivery applications: imaging, targeting, and delivery*. Springer Science & Business Media: 2012.
24. Gavrilov, K.; Saltzman, W. M., Therapeutic siRNA: principles, challenges, and strategies. *The Yale journal of biology and medicine* **2012,** *85* (2), 187.
25. Shen, H.; Sun, T.; Ferrari, M., Nanovector delivery of siRNA for cancer therapy. *Cancer gene therapy* **2012,** *19* (6), 367.
26. Dowdy, S. F., Overcoming cellular barriers for RNA therapeutics. *Nature biotechnology* **2017,** *35* (3), 222.
27. O'Mahony, A. M.; Godinho, B. M. D. C.; Cryan, J. F.; O'Driscoll, C. M., Non-Viral Nanosystems for Gene and Small Interfering RNA Delivery to the Central Nervous System: Formulating the Solution. *Journal of pharmaceutical sciences* **2013,** *102* (10), 3469-3484.
28. M O'Mahony, A.; J O'Neill, M.; Mdc Godinho, B.; Darcy, R.; F Cryan, J.; M O'Driscoll, C., Cyclodextrins for non-viral gene and siRNA delivery. *Pharmaceutical Nanotechnology* **2013,** *1* (1), 6-14.
29. Sallas, F.; Darcy, R., Amphiphilic cyclodextrins–advances in synthesis and supramolecular chemistry. *European Journal of Organic Chemistry* **2008,** *2008* (6), 957-969.

30. O'Mahony, A. M.; Ogier, J.; Desgranges, S.; Cryan, J. F.; Darcy, R.; O'Driscoll, C. M., A click chemistry route to 2-functionalised PEGylated and cationic β-cyclodextrins: co-formulation opportunities for siRNA delivery. *Organic & biomolecular chemistry* **2012,** *10* (25), 4954-4960.
31. Godinho, B. M. D. C.; Ogier, J. R.; Quinlan, A.; Darcy, R.; Griffin, B. T.; Cryan, J. F.; O'Driscoll, C. M., PEGylated cyclodextrins as novel siRNA nanosystems: correlations between polyethylene glycol length and nanoparticle stability. *International journal of pharmaceutics* **2014,** *473* (1-2), 105-112.
32. Gooding, M.; Malhotra, M.; McCarthy, D. J.; Godinho, B. M. D. C.; Cryan, J. F.; Darcy, R.; O'driscoll, C. M., Synthesis and characterization of rabies virus glycoprotein-tagged amphiphilic cyclodextrins for siRNA delivery in human glioblastoma cells: in vitro analysis. *European Journal of Pharmaceutical Sciences* **2015,** *71*, 80-92.
33. Cryan, S. A.; Donohue, R.; Ravoo, B. J.; Darcy, R.; O'Driscoll, C. M., Cationic cyclodextrin amphiphiles as gene delivery vectors. *Journal of Drug Delivery Science and Technology* **2004,** *14* (1), 57-62.
34. McMahon, A.; O'Neill, M. J.; Gomez, E.; Donohue, R.; Forde, D.; Darcy, R.; O'Driscoll, C. M., Targeted gene delivery to hepatocytes with galactosylated amphiphilic cyclodextrins. *Journal of Pharmacy and Pharmacology* **2012,** *64* (8), 1063-1073.
35. Godinho, B. M. D. C.; Ogier, J. R.; Darcy, R.; O'Driscoll, C. M.; Cryan, J. F., Self-assembling modified β-cyclodextrin nanoparticles as neuronal siRNA delivery vectors: Focus on Huntington's disease. *Molecular pharmaceutics* **2013,** *10* (2), 640-649.
36. McCarthy, J.; O'Neill, M. J.; Bourre, L.; Walsh, D.; Quinlan, A.; Hurley, G.; Ogier, J.; Shanahan, F.; Melgar, S.; Darcy, R., Gene silencing of TNF-alpha in a murine model of acute colitis using a modified cyclodextrin delivery system. *Journal of controlled release* **2013,** *168* (1), 28-34.
37. Guo, J.; Russell, E. G.; Darcy, R.; Cotter, T. G.; McKenna, S. L.; Cahill, M. R.; O'Driscoll, C. M., Antibody-targeted cyclodextrin-based nanoparticles for siRNA delivery in the treatment of acute myeloid leukemia: physicochemical characteristics, in vitro mechanistic studies, and ex vivo patient derived therapeutic efficacy. *Molecular pharmaceutics* **2017,** *14* (3), 940-952.
38. Godinho, B. M. D. C.; McCarthy, D. J.; Torres-Fuentes, C.; Beltrán, C. J.; McCarthy, J.; Quinlan, A.; Ogier, J. R.; Darcy, R.; O'Driscoll, C. M.; Cryan, J. F., Differential nanotoxicological and neuroinflammatory liabilities of non-viral vectors for RNA interference in the central nervous system. *Biomaterials* **2014,** *35* (1), 489-499.
39. Villari, V.; Mazzaglia, A.; Darcy, R.; O'Driscoll, C. M.; Micali, N., Nanostructures of cationic amphiphilic cyclodextrin complexes with DNA. *Biomacromolecules* **2013,** *14* (3), 811-817.
40. O'Mahony, A. M.; Cronin, M. F.; McMahon, A.; Evans, J. C.; Daly, K.; Darcy, R.; O'Driscoll, C. M., Biophysical and structural characterisation of nucleic Acid complexes with modified cyclodextrins using circular dichroism. *Journal of pharmaceutical sciences* **2014,** *103* (5), 1346-1355.
41. Meneksedag-Erol, D.; Tang, T.; Uludağ, H., Molecular modeling of polynucleotide complexes. *Biomaterials* **2014,** *35* (25), 7068-7076.
42. Nash, J. A.; Kwansa, A. L.; Peerless, J. S.; Kim, H. S.; Yingling, Y. G., Advances in Molecular Modeling of Nanoparticle–Nucleic Acid Interfaces. *Bioconjugate chemistry* **2016,** *28* (1), 3-10.
43. Karthik, S.; Thirugnanasambandam, A.; Mandal, P. K.; Gautham, N., Comparison of X-ray crystal structures of a tetradecamer sequence d (CCCGGGTACCCGGG) 2 at 1.7 Å resolution. *Nucleosides, Nucleotides and Nucleic Acids* **2017,** *36* (5), 343-354.
44. Hardwick, J. S.; Ptchelkine, D.; El-Sagheer, A. H.; Tear, I.; Singleton, D.; Phillips, S. E. V.; Lane, A. N.; Brown, T., 5-Formylcytosine does not change the global structure of DNA. *Nature structural & molecular biology* **2017,** *24* (6), 544.
45. Purushothaman, M.; Varghese, A.; Mandal, P. K.; Gautham, N., Structure of d (CCCCGGTACCGGGG) 2 at 1.65 Å resolution. *Acta Crystallographica Section F: Structural Biology Communications* **2014,** *70* (7), 860-865.
46. Mandal, P. K.; Venkadesh, S.; Gautham, N., Structure of the tetradecanucleotide d

(CCCCGGTACCGGGG) 2 as an A-DNA duplex. *Acta Crystallographica Section F: Structural Biology and Crystallization Communications* **2012,** *68* (4), 393-399.
47. Schmidt, A. K.; Cottaz, S.; Driguez, H.; Schulz, G. E., Structure of cyclodextrin glycosyltransferase complexed with a derivative of its main product β-cyclodextrin. *Biochemistry* **1998,** *37* (17), 5909-5915.
48. Jorgensen, W. L.; Chandrasekhar, J.; Madura, J. D.; Impey, R. W.; Klein, M. L., Comparison of simple potential functions for simulating liquid water. *The Journal of chemical physics* **1983,** *79* (2), 926-935.
49. Darden, T.; York, D.; Pedersen, L., Particle mesh Ewald: An N· log (N) method for Ewald sums in large systems. *The Journal of chemical physics* **1993,** *98* (12), 10089-10092.
50. Hess, B., P-LINCS: A parallel linear constraint solver for molecular simulation. *Journal of Chemical Theory and Computation* **2008,** *4* (1), 116-122.
51. Parrinello, M.; Rahman, A., Polymorphic transitions in single crystals: A new molecular dynamics method. *Journal of Applied physics* **1981,** *52* (12), 7182-7190.
52. Nosé, S.; Klein, M. L., Constant pressure molecular dynamics for molecular systems. *Molecular Physics* **1983,** *50* (5), 1055-1076.
53. Vanommeslaeghe, K.; Hatcher, E.; Acharya, C.; Kundu, S.; Zhong, S.; Shim, J.; Darian, E.; Guvench, O.; Lopes, P.; Vorobyov, I., CHARMM general force field: A force field for drug-like molecules compatible with the CHARMM all-atom additive biological force fields. *Journal of computational chemistry* **2010,** *31* (4), 671-690.
54. Denning, E. J.; Priyakumar, U. D.; Nilsson, L.; Mackerell, A. D., Impact of 2 '-Hydroxyl Sampling on the Conformational Properties of RNA: Update of the CHARMM All-Atom Additive Force Field for RNA. *Journal of Computational Chemistry* **2011,** *32* (9), 1929-1943.
55. Huang, J.; MacKerell Jr, A. D., CHARMM36 all-atom additive protein force field: Validation based on comparison to NMR data. *Journal of computational chemistry* **2013,** *34* (25), 2135-2145.
56. Guvench, O.; Mallajosyula, S. S.; Raman, E. P.; Hatcher, E.; Vanommeslaeghe, K.; Foster, T. J.; Jamison, F. W.; MacKerell, A. D., CHARMM Additive All-Atom Force Field for Carbohydrate Derivatives and Its Utility in Polysaccharide and Carbohydrate–Protein Modeling. *Journal of Chemical Theory and Computation* **2011,** *7* (10), 3162-3180.
57. Best, R. B.; Zhu, X.; Shim, J.; Lopes, P. E. M.; Mittal, J.; Feig, M.; MacKerell, A. D., Jr., Optimization of the Additive CHARMM All-Atom Protein Force Field Targeting Improved Sampling of the Backbone phi, psi and Side-Chain chi(1) and chi(2) Dihedral Angles. *Journal of Chemical Theory and Computation* **2012,** *8* (9), 3257-3273.
58. Abraham, M. J.; Murtola, T.; Schulz, R.; Páll, S.; Smith, J. C.; Hess, B.; Lindahl, E., GROMACS: High performance molecular simulations through multi-level parallelism from laptops to supercomputers. *SoftwareX* **2015,** *1*, 19-25.
59. Pronk, S.; Páll, S.; Schulz, R.; Larsson, P.; Bjelkmar, P.; Apostolov, R.; Shirts, M. R.; Smith, J. C.; Kasson, P. M.; Van Der Spoel, D., GROMACS 4.5: a high-throughput and highly parallel open source molecular simulation toolkit. *Bioinformatics* **2013,** *29* (7), 845-854.
60. Lu, Y.; Li, J.; Su, N.; Lu, D., The Mechanism for siRNA Transmembrane Assisted by PMAL. *Molecules* **2018,** *23* (7), 1586.
61. Manzanares, D.; Araya-Duran, I.; Gallego-Yerga, L.; Jativa, P.; Marquez-Miranda, V.; Canan, J.; Blanco, J. L. J.; Mellet, C. O.; Gonzalez-Nilo, F. D.; Fernandez, J. M. G.; Cena, V., Molecular determinants for cyclooligosaccharide-based nanoparticle-mediated effective siRNA transfection. *Nanomedicine* **2017,** *12* (13), 1607-1621.
62. Shen, J. W.; Li, J. C.; Zhao, Z. N.; Zhang, L.; Peng, G. T.; Liang, L. J., Molecular dynamics study on the mechanism of polynucleotide encapsulation by chitosan. *Scientific Reports* **2017,** *7*, 9.
63. Li, J.; Ouyang, Y.; Kong, X.; Zhu, J.; Lu, D.; Liu, Z., A multi-scale molecular dynamics simulation of PMAL facilitated delivery of siRNA. *RSC Advances* **2015,** *5* (83), 68227-68233.
64. Lu, Y.; Li, J.; Lu, D., The mechanism for the complexation and dissociation between siRNA

and PMAL: a molecular dynamics simulation study based on a coarse-grained model. *Mol. Simul.* **2017,** *43* (13-16), 1385-1393.

65. Chang, P. K. C.; Prestidge, C. A.; Bremmell, K. E., Interfacial analysis of siRNA complexes with poly-ethylenimine (PEI) or PAMAM dendrimers in gene delivery. *Colloid Surf. B-Biointerfaces* **2017,** *158*, 370-378.

66. Krivitsky, A.; Krivitsky, V.; Polyak, D.; Scomparin, A.; Eliyahu, S.; Gibori, H.; Yeini, E.; Pisarevsky, E.; Blau, R.; Satchi-Fainaro, R., Molecular Weight-Dependent Activity of Aminated Poly()glutamates as siRNA Nanocarriers. *Polymers* **2018,** *10* (5), 22.